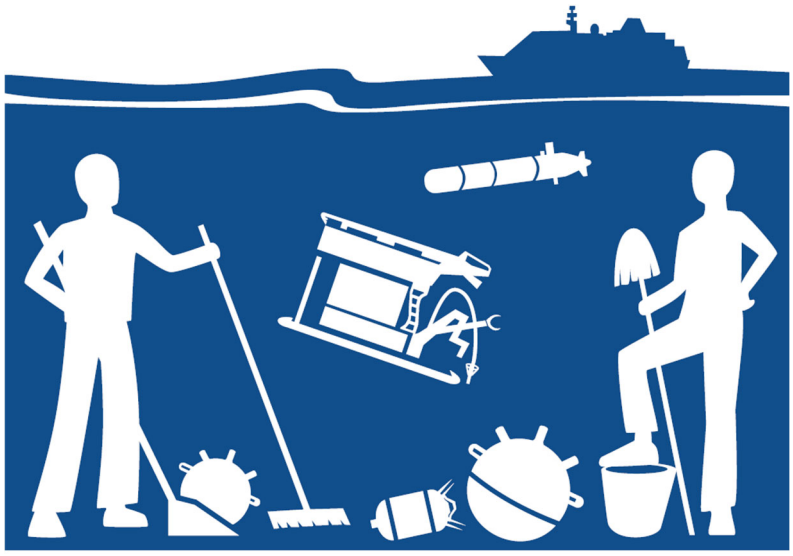

MMinE-SwEEPER

Deliverable Report

Deliverable No. 8.5: CWA analyses through NAA

Funded by
the European Union

Authors | Grzegorz Siedlewicz, Ewa Korejwo, Jacek Bełdowski

Contributing organisations:

DOCUMENT TRACKING DETAILS

Project Information

Project acronym	MMinE-SwEEPER
Project title	Marine Munition in Europe - Solutions with Economic and Ecological Profits for Efficient Remediation
Instrument	Horizon Europe
Grant Agreement	No. 101167839
Starting date	1 October 2024
Duration	31 March 2028
Project Coordinator	GEOMAR Helmholtz Centre for Ocean Research Kiel

Deliverable Information

Deliverable Name	CWA analyses through NAA
Deliverable Number	D8.5
Work Package (WP)	8
Related Task (s)	8.3
Deliverable Beneficiary	Institute of Oceanology Polish Academy of Sciences (IO PAN)
Author(s)	Grzegorz Siedlewicz, Ewa Korejwo, Jacek Bełdowski
Due date	31 March 2026
Submission date	31 March 2026
Type of deliverable	Report
Dissemination level	PU

Acknowledgements

This report was produced by Institute of Oceanology Polish Academy of Sciences (IO PAN) in the scope of the MMinE-SwEEPER project. This project has received funding from the European Union's Horizon Europe Research and Innovation Programme under Grant Agreement No. 101167839.

Disclaimer

Funded by the European Union. Views and opinions expressed are however those of the author(s) only and do not necessarily reflect those of the European Union or the European Research Executive Agency. Neither the European Union nor the granting authority can be held responsible for them.

This document contains information on MMinE-SwEEPER's core activities. Any reference to content in this document should clearly indicate the authors, source, organisation, and publication date.

Contact details

Questions, comments, and/or concerns about this document should be emailed to Grzegorz Siedlewicz at gsiedlewicz@iopan.pl, subject line "MMinE-SwEEPER Deliverable 8.5 CWA analyses through NAA".

Contents

List of figures

List of tables

1. Introduction

1.1 The environmental and security challenge of sea-dumped chemical warfare agents

The legacy of sea-dumped chemical weapons (CW) represents a complex, multi-dimensional hazard affecting the marine environment, human health, and maritime security. Following the conclusion of both World Wars, the global community was faced with the immediate necessity of disposing of massive stockpiles of surplus and captured chemical warfare agents (CWA). Between 1919 and 1970, deep-sea dumping was considered the most efficient and cost-effective disposal method, based on the then-prevailing scientific assumption that the vastness of the ocean would dilute any leakages to negligible levels (**Bełdowski et al., 2018**). The scale of the problem is global (**Figure 1**). The total quantity of CW material is estimated for at least 1.6 million tons (**Wilkinson et al., 2017**).
In the European theater, the Potsdam Agreement of 1945 served as a primary catalyst for these operations. Under the mandate to disarm Germany, Allied powers utilized sea disposal for captured stocks. British and American authorities primarily utilized the Skagerrak strait, while Soviet authorities directed dumping operations into the Baltic Proper (**Söderström et al., 2018**). In the Baltic Sea alone, at least 50,000 tons of CW were dumped, containing roughly 15,000 tons of pure chemical warfare agents. Key identified sites include the Bornholm Deep, the Gotland Basin, and the Little Belt. Disposal methods varied from scuttling entire ships loaded with chemical cargo to "item-by-item" disposal, where munitions were manually jettisoned from vessels en route to designated areas. This practice led to the creation of unofficial dumpsites along transport routes, significantly complicating modern mapping and monitoring efforts (**Bełdowski et al., 2018**).

The CWA problem are defined by the specific chemical properties of the agents and their degradation pathways under high pressure, low temperature, and varying salinity. The primary categories of concern identified in major research initiatives such as the MODUM and CHEMSEA projects include:

- Sulfur Mustard (HD/Yperite): Quantitatively the most significant agent in the Baltic. It is a blistering agent with low water solubility. In marine settings, it frequently undergoes surface polymerization, forming a "mustard heel" or lumps with a protective crust. This crust can shield an active, liquid core for over 50 years, posing an acute risk to fishermen who may accidentally recover these lumps in trawling nets (**Söderström et al., 2018**).

- Arsenic-based Agents: These include Clark I, Clark II, and Adamsite. Unlike mustard gas, these compounds hydrolyze rapidly but result in persistent organoarsenic species. Because arsenic is not naturally abundant in such concentrated forms, its detection in sediment serves as a critical inorganic marker for leaking munitions. High concentrations (up to 210–277 μg/g) have been recorded in fine-grained sediments near dumpsites (**Söderström et al., 2018**).

- Nerve Agents: While less common than blister agents, organophosphates like Tabun (GA) were dumped in specific locations. These agents are generally more soluble and hydrolyze faster than mustard gas, yet their presence continues to be a focus of toxicity studies (**Söderström et al., 2018**).

- Munition Casings and Conventional Explosives: The steel shells are subject to chronic corrosion, with rates estimated between 0.05 to 0.575 mm/year (**Bełdowski et al., 2018**). Furthermore, most chemical munitions contain conventional explosives (TNT, DNT) used as burster charges, which add a secondary layer of toxic stress to the environment.

Once the integrity of a munition casing is breached, the contents enter the sediment-water interface. The environmental fate of these chemicals is governed by complex advection and diffusion processes. In the deep basins of the Baltic, which are often characterized by permanent haloclines and stagnant, hypoxic (low oxygen) conditions, the dispersion of agents like mustard gas may be localized. However, arsenic-based agents have been observed to spread further from the source (**Bełdowski et al., 2018**). The biological consequences are profound. Research indicates that benthic communities in dumpsites—such as meiofaunal nematodes—exhibit altered abundance and diversity, potentially as a response to chemical stress. Furthermore, demersal fish like the Atlantic Cod (*Gadus morhua*) are at risk of chronic exposure (**Lang et al., 2018**).

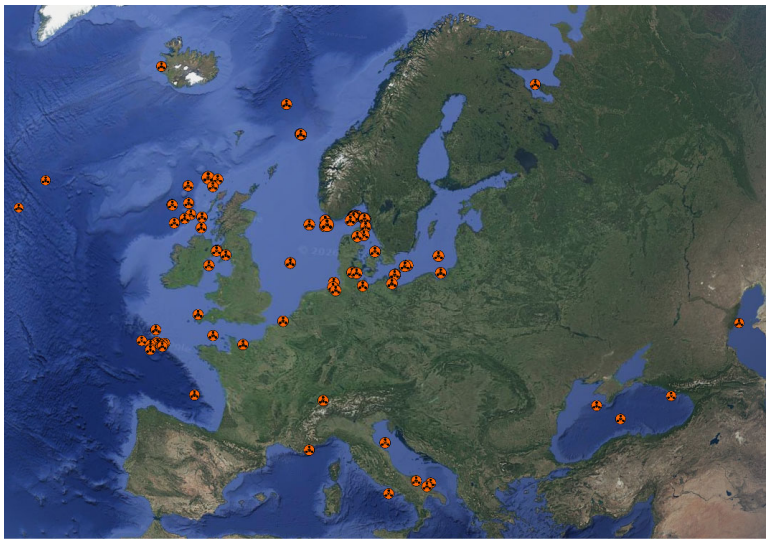

Figure 1 Chemical munitions dumped in the seas. Copyright by James Martin, Centre for Non-proliferation studies (**Wilkinson et al., 2017**).

1.2 The EU context

The systematic evaluation of CWA as a primary trans-border environmental risk was initiated under a NATO pilot study in 1992, subsequently leading to the establishment of the HELCOM committees CHEMU and MUNI to address CWA remnants in the Baltic Sea (**HELCOM, 1995, 2013**). Over the past two decades, EU-funded and national research initiatives have prioritized the detection and characterization of CWA dumpsites to assess their long-term ecological impact. Early foundational work was conducted under the REDCOD program (2002–2005), which provided an initial assessment of environmental damage caused by chemical ordnance (**Amato et al., 2006**). This was followed by the MERCW project (2003–2008), which focused on the complex modelling of ecological risks associated with submerged chemical weapons (**Stipa and Paka, 2006**).

More recently, the CHEMSEA project (2011–2013) significantly advanced the mapping of CWA contaminated areas and the assessment of their toxicity to marine organisms (**Bełdowski et al., 2016**). Building upon these findings, the NATO MODUM project (2013–2016) established advanced standard operating procedures for the continuous monitoring of CWA degradation products using underwater vehicles and in situ analytical techniques (**Bełdowski et al., 2018**). These collective efforts have shifted the focus towards decision-support frameworks, such as the DAIMON project, which evaluates the chemical stability and biological exposure risks of CWA remnants. Collectively, these studies have conclusively demonstrated that CWA leakage is a persistent phenomenon in EU marine waters, with measurable concentrations of degradation products evident in both the sediment-water interface and the marine biota.

1.3 Operational and safety drivers for on-board CWA analysis

Environmental sampling near submerged munitions is conducted to investigate potential chemical leakage, yet executing these operations at depths of 100 meters presents significant technical and safety challenges. Precise targeting is difficult, and there is a persistent risk of the sampling gear inadvertently striking a high-toxicity object. This is complicated by the advanced state of corrosion of many dumped items; for instance, sulfur mustard often polymerizes into solidified masses that are indistinguishable from natural seafloor features. Given the high operational costs associated with research vessels and specialized personnel, the ability to perform "on-site" detection of mustard-related degradation products is invaluable. Immediate shipboard analysis allows for the implementation of safe sample handling protocols and enables the crew to dynamically redirect sampling efforts toward confirmed "hot spots" (**Fish et al., 2010; Söderström et al., 2018**).

Furthermore, the implementation of ruggedized laboratory instrumentation on research vessels provides the necessary sensitivity and selectivity to identify relevant wrecks and munitions during the mission. This real-time capability ensures that field teams focus their resources on objects of high environmental significance. While these shipboard results provide immediate operational guidance, they serve as a preliminary phase that is subsequently validated in land-based "reach-back" laboratories. There, sediment extracts undergo rigorous analysis using high-resolution hyphenated techniques, such as GC–MS/MS and LC–HRMS, to confirm the identity and precise concentration of the contaminants (**Söderström et al., 2018**).

The aim of this report is to compile current knowledge on state-of-the-art chemical warfare agent analysis, with a specific emphasis on the methodologies developed during the NATO MODUM project to enhance operator security during clearance operations. Furthermore, the task focuses on advancing a novel neutron activation analyser (NAA) for the non-invasive identification and classification of chemical versus conventional munitions, while establishing the technical requirements for its deployment via remotely operated vehicles (ROV).

2. On-board CWA analysis

Informations in presented chapter are synthesis of the results implemented in NATO Modum project. The analyses were made for Baltic Sea but can be transferred to other regions like Black Sea, North Sea and/or Mediterranean Sea.

2.1 Hazmat-teams/CBRN-units

Preliminary screening of marine samples can be conducted using portable detection equipment originally designed for military CBRN (Chemical, Biological, Radiological, and Nuclear) and Hazmat units. However, these tools must be utilized with significant caution when assessing legacy underwater munitions due to their specific operational limitations **(Söderström et al., 2018).**

A primary challenge is the lack of specificity in certain detection technologies. For instance, flame photometric detectors like the AP2C which is hydrogen flame spectrometer detector designed for fully automatic operation in field conditions **(Figure 2)**. It is capable of detecting a wide range of both conventional and unconventional chemical threats, providing rapid and reliable results without the need for manual intervention. The device is used to detect, classify, and estimate the concentration of chemical warfare agents (CWAs) and toxic industrial substances (TIS) in the air. It can also identify these substances in liquid samples, including water, as well as in solid materials. Owing to its high sensitivity, the AP4C is widely applied in evaluating the effectiveness of decontamination processes for weapons, military equipment, and exposed body surfaces. The problem with detection is that the AP2C identify elemental sulfur; while this is a marker for sulfur mustard, it can also yield false positives by detecting hydrogen sulfide produced naturally through anaerobic microbial activity in marine sediments. Similarly, although Ion Mobility Spectrometry (IMS) is effective at alerting teams to the

presence of concentrated, active chemical agents during a direct encounter with a munition, it is generally inadequate for broader environmental assessments. This is because contaminated sediments typically contain CWA degradation products—primarily hydrolysis derivatives—at parts-per-billion (ppb) concentrations, which fall below the detection thresholds or outside the analytical scope of standard military-grade sensors **(Söderström et al., 2018)**.

Figure 2 The automatic chemical detection device (AP4C) (Photo by Marita Ljønes).

2.2 Analysis of CWA with deployable headspace GC–MS

The deployment of analytical chemistry in the context of marine munition surveys requires a tiered approach that balances the need for rapid, field-based decision-making with the rigorous precision of land-based forensic laboratories. The primary instrument utilized for on-site screening during the MODUM project was a ruggedized gas chromatography-mass spectrometry (GC–MS) system. Originally engineered for use by first responders and hazardous material units, this system incorporates specialized software, such as the Automatic Mass spectral Deconvolution and Identification Software (AMDIS), which enables the automated processing of complex data files. This automation allows sampling teams with limited analytical experience to achieve rapid data interpretation, providing immediate results that are critical for operational safety. The software, initially developed as a tool for verifying compliance with the Chemical Weapons Convention (CWC), is highly adaptable and can be calibrated for a wide array of compounds detectable via gas chromatography **(Söderström et al., 2018).**

Operational efficiency on a research vessel is often dictated by the ability to minimize specialized personnel; therefore, it is preferred that the sampling team operates the analytical hardware directly. For these operators, the identification of target chemicals relies on automated data convolution, utilizing linear retention indices and spectral match factors that must exceed eighty-five percent to ensure reliability. While the technological constraints of ruggedized hardware often result in broader

chromatographic peaks compared to benchtop equivalents, the resulting quadrupole full-scan mass spectrometry data remains highly effective for the intended purpose of field screening. Under automated identification parameters, the system typically achieves detection limits between fifteen and eighty parts-per-billion (ppb). However, when field-collected data files are transmitted to experienced chemists for secondary processing, these limits can be further reduced to a range of two to ten ppb. This expert-level analysis also allows for the semi-quantification of contaminants through the use of internal standards added during the initial field sampling phase **(Söderström et al., 2018).**

The specific methodology optimized for on-ship analysis is the headspace trap GC–MS technique, which represents a significant departure from standard first-responder protocols **(Figure 3)**. Achieving parts-per-billion sensitivity for sulfur mustard markers in marine sediment requires the meticulous optimization of every analytical stage. To maintain the flow of maritime operations, sample manipulation is kept to a minimum, with centrifugation serving as the sole preparation step to isolate the sediment fraction from its pore water. This approach is essential because World War II-era munitions often contain not only primary agents but also a variety of additives and secondary compounds that serve as forensic fingerprints. For instance, German munitions frequently utilized arsine oil—composed of various phenyl arsines—to lower the freezing point of sulfur mustard, whereas American and Russian stockpiles often incorporated Lewisite for the same purpose **(BSH, 1993)**. The detection of these additives, alongside vomiting agents like Adamsite and lachrymators such as Clark I and II, provides indispensable information regarding the origin and national provenance of the dumped material. **(Söderström et al., 2018)**.

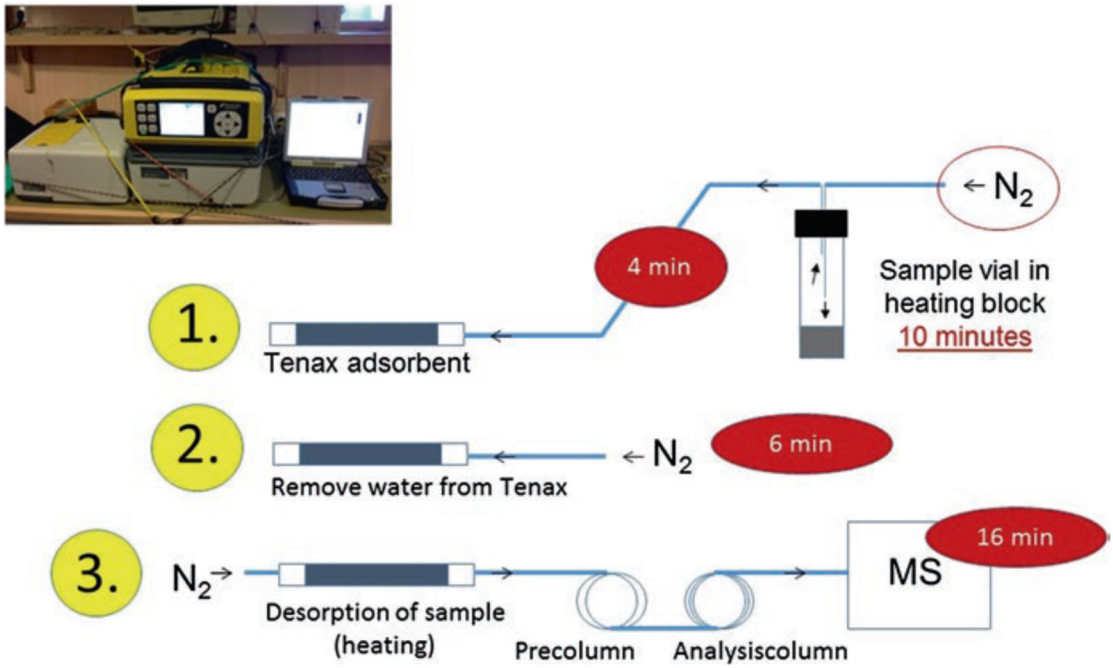

Figure 3 Headspace analysis principle: (1) Headspace vapour from preheated sample is concentrated on an in built tenax concentrator tube, (2) excess of accumulated water on the Tenax concentrator from sampling has to be removed with drying gas (N2) optimised to minimize the losses of analytes, (3) desorption and GC–MS analysis (Fig. after **Söderström et al., 2018**).

2.3 Analysis of CWA by portable capillary electrophoresis

Capillary electrophoresis (CE) is an advanced analytical technique designed to separate ions by utilizing an applied voltage to drive their migration based on electrophoretic mobility. The separation process occurs within a narrow-bore capillary, typically featuring an inner diameter of 10–100 µm. The fundamental mechanism of CE relies on two distinct electrokinetic phenomena: electrophoresis and electroosmosis. The speed and efficiency of the separation are governed by several key physical

parameters. Specifically, electrophoretic mobility is determined by the electric charge of the molecule, the viscosity of the background electrolyte (BGE), and the radius of the atom or particle. Because the velocity of a particle is directly proportional to the strength of the applied electric field, higher field strengths result in faster migration rates **(Li, 1992)**. For on-site analysis, conductivity detection—and specifically capacitively coupled contactless conductivity detection (C4D)—is considered the most appropriate for on-site analysis due to its minimal power consumption and high sensitivity toward nerve agent degradation products **(Kubáň et al., 2011; Söderström et al., 2018)**.

Within the framework of the NATO MODUM project, the research group from Tallinn University of Technology (TTÜ) focused on developing and validating analytical protocols to detect the degradation products of both mustards and nerve agents in seawater and sediment pore-water. The group utilized a custom-developed portable CE−C4D instrument characterized by its compact dimensions (30×30×15 cm) and low mass (3.5 kg), which allowed for rapid and easy transportation to research vessels **(Figure 4)**. The applied methodologies achieved limits of detection (LOD) between 6.8–19.8 µM for five nerve agent hydrolysis products and 4.1–5.2 µM for three nitrogen mustard derivatives (EDEA, MDEA, and TEA), building upon established protocols in the literature **(Seiman et al., 2009; Kubáň et al., 2011).**

Figure 4 A portable CE-C4D instrument (Fig. after **Söderström et al., 2018**).

In aqueous environments, sulfur mustard hydrolyzes into thiodiglycol (TDG) and its subsequent oxidation products, thiodiglycol sulfoxide (TDGO) and thiodiglycol sulfone (TDGOO). The TTÜ team successfully implemented CE protocols that achieved baseline separation of these three derivatives in less than 8 minutes using a borate buffer as the background electrolyte. This method provided LODs in the range of 98–154 ng/mL and was successfully applied to seawater and pore-water samples using carbon aerogel-based adsorbents for sample purification **(Jõul et al., 2015)**. Further advancements led to a portable method for the simultaneous determination of six different hydrolysis products from both nitrogen and sulfur mustards. While the sample preparation involving solid-phase extraction and derivatization with phthalic anhydride remains time-consuming, the electrophoretic separation itself is completed in under 15 minutes **(Kubáň et al., 2011)**.

The practical utility of this technology was demonstrated during the MODUM cruise aboard the R/V Oceania in March 2016 in the Bornholm Basin. The portable CE−C4D instrument exhibited full operational robustness in the maritime environment. Although the specific pore-water samples analyzed on board showed no traces of contamination, these results were definitively confirmed through subsequent laboratory re-analysis using stationary CE−UV instrumentation **(Figure 5)**. In conclusion, while capillary electrophoresis is not yet the most common technique for identifying CWA

degradation products, it represents a highly viable solution due to its simplicity, robustness, and the possibility of utilizing in-line pre-concentration to enhance detection limits in real environmental samples **(Söderström et al., 2018).**

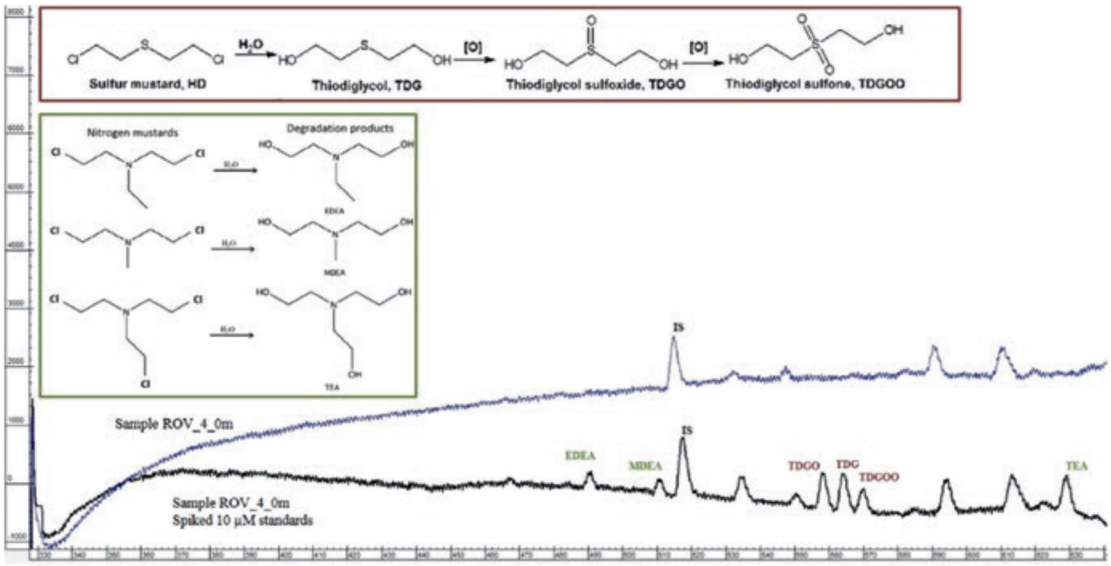

Figure 5 Representative electropherograms obtained from the MODUM Bornholm cruise in March 2016 and a sulfur and nitrogen mustards degradation pathways (Fig. after **Söderström et al., 2018**).

3. Neutron Activation Analysis NAA

The following section discusses the potential application of Neutron Activation Analysis (NAA) for the detection of munition constituents in the marine environment, expanding upon the methodologies previously described in Chapter 2, which relied on established techniques and commercially available equipment. The information presented in this section is derived from the "Final Report on Commissioned Research No. K/KDU/000990: Research on the Suitability of Neutron Activation Analysis for the Identification of Chemical Warfare Agents," authored by M. Silarski, M. Kaczmarek, K. Dulski, and W. Zantowicz from the Faculty of Physics, Astronomy, and Applied Computer Science at the Jagiellonian University. This report was prepared as a commissioned document, and the costs associated with the research were fully covered under the framework of the MMinE-SwEEPER project. The research consists of theoretical and practical parts. The theoretical part included a Monte Carlo simulation of an NAA-based sensor consisting of a neutron generator and a gamma quantum detector installed on an ROV (remotely operated vehicle). The simulation results show the expected energy spectra obtained in the gamma-ray detector. These spectra were then used to determine the optimal set of gamma lines for the activated isotopes of the tested substances, enabling their identification. The report describes changes in the sensor's performance as a function of distance from the substance under investigation and the thickness of bomb and missile shells and ship hulls, demonstrating how the thickness of the hull and tank affects detection quality. Based on the simulations, it was verified whether modifying the DT neutron generator—by correlating measurements in the gamma quantum detector with alpha particle measurements—improves the time separation of gamma quanta from inelastic scattering and neutron capture. The experimental part of this research contained irradiation studies of selected substances: melamine (an explosives surrogate), a sample of the Baltic Sea bottom, NaCl (a surrogate of the chlorine signal), and water (a reference) in conditions simulating the aquatic environment. Elemental ratios for seven lines

corresponding to hydrogen, oxygen, carbon, and chlorine were studied in view of the influence of water and steel shells covering the examined material.

3.1 Monte Carlo simulations

Monte Carlo simulations were performed using dedicated software developed for the SABAT project, based on the Geant4 **(Allison et al., 2016)** and ROOT **(Brun and Rademakers, 1997)** libraries. The designed system in the simulations consisted of a neutron generator and a detection system placed in the arms of ROV, which were aimed at the tested object as shown in **Figure 6**. The point source of neutrons was located in a generator made of low-carbon steel, 3 mm thick and measuring 10.8 x 20.3 x 25.4 cm, located at the end of the right arm of the ROV. Each event started with the isotropic emission of a 14.1 MeV neutron and a 3.49 MeV alpha particle in the opposite direction to the neutron. Additionally, in the generator volume, 5 cm from the source, a silicon detector was added, tagging an alpha particle with dimensions of 8 x 8 x 0.1 cm. The second arm of the ROV houses a detection system consisting of a LaBr scintillator in the form of a 2" x 2" cylinder and silicon detectors attached to the rear wall of the scintillator. The ROV was designed as a cuboid measuring 215 x 116 x 125.3 cm with two cylindrical arms measuring 6.25 x 68.6 cm.

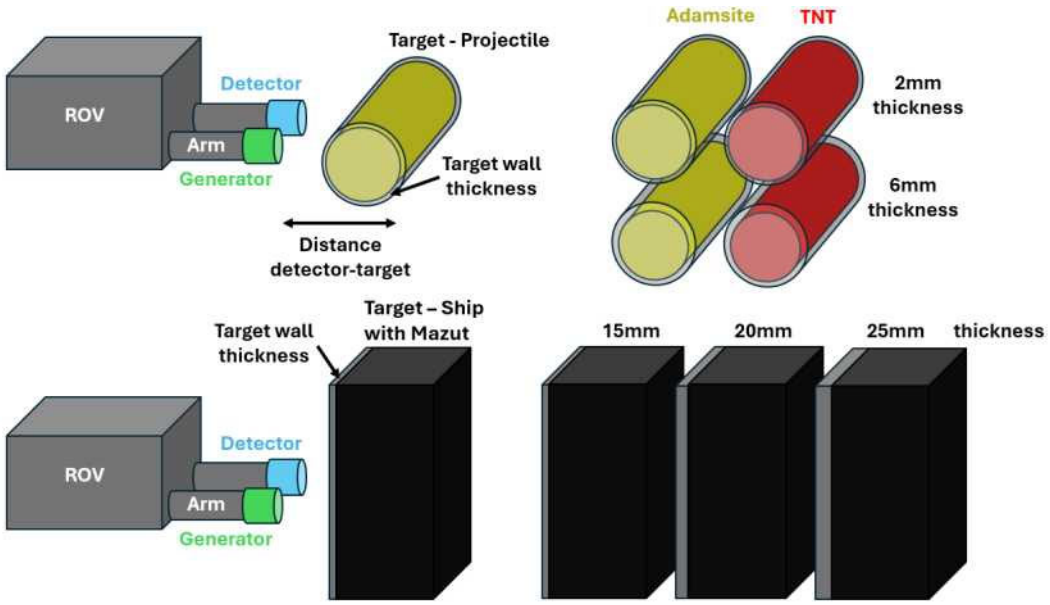

Figure 6 Scheme of the simulation setup with two different types fo the target - projectile (cylinder) and ship (cu-boid). Two dangerous materials were simulated in the projectile - Adamsite and TNT, while the fuel in the ship was simulated in the form of Mazut. During the simulation, two main parameters were changed - the thickness of the target wall and the distance between the detector and the target.

Two designs of the tested targets were selected: a projectile and a ship wall. TNT and Adamsite were simulated in the projectile, and heavy fuel oil (mazut) in the ship. Additionally, simulations with water inside the projectile and ship, respectively, were used as reference materials. ST42 steel was used for the walls of the projectile and ship. The simulation was performed for two projectile thicknesses (2 and 6 mm) and three ship thicknesses (15, 20, 25 mm), as well as for four different distances between the tested object and the end of the ROV arms (0, 20, 40 and 60 cm). For each configuration: object type, material inside, wall thickness, and distance, 5E8 events were simulated. The simulation data were then analyzed using dedicated software to collect the energy distribution for all of the detected events. In addition to the photon energy after interaction with neutrons, the distributions of the photon arrival time at the detector were also collected.

3.1.1. Analysis details

The simulated energy distribution for each material and configuration was fitted using a signal model consisting of a sum of Gaussians with fixed offsets corresponding to the characteristic energies expected in the distribution based on the isotopic composition. Additionally, a model based on a combination of exponential and broad Gaussian distributions was used to estimate the background, to cover energies not originating from the characteristic radiation from the neutron-matter interaction, as well as photons that did not deposit their full energy in the detector. The fits were performed in dedicated software for the previously described simulations (SABAT MC]) in the ROOT environment **(Brun and Rademakers, 1997)** and based on the Minuit2 algorithm. An example decomposition with separation into contribution from signal and background is shown in **Figure 7**.

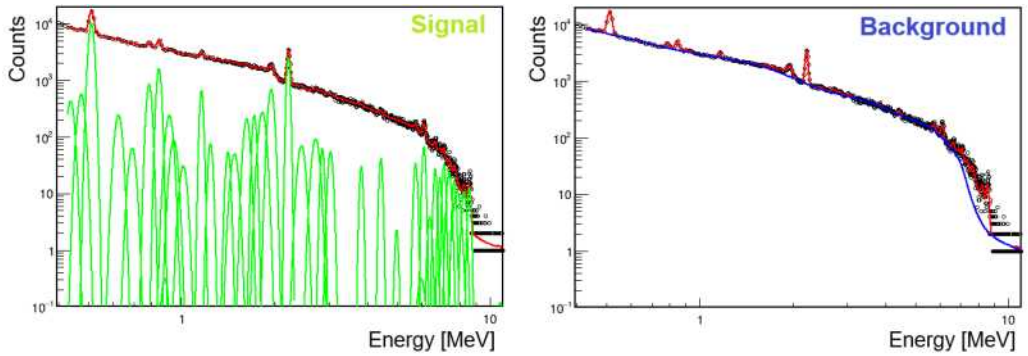

Figure 7 Exemplary fit of the energy distribution from which the intensity for each line is obtained. Spectrum is separated onto signal and background, where the intensity for each line is then subjected to further analysis.

3.1.2 Simulation results

The energy distributions from the simulation for a projectile-type object for Adamsite and TNT with two different wall thicknesses and for different distances from the target can be seen in **Figure 8**. For an object like a ship with mazut behind the walls are shown in **Figure 9**. All distributions are shown against the background of results for the same configurations but with the target material replaced by water, treated as the reference material in this analysis. It is worth noting how increasing the distance from the target eliminates the differences between simulations with a given material (Adamsite, TNT and mazut) and water.

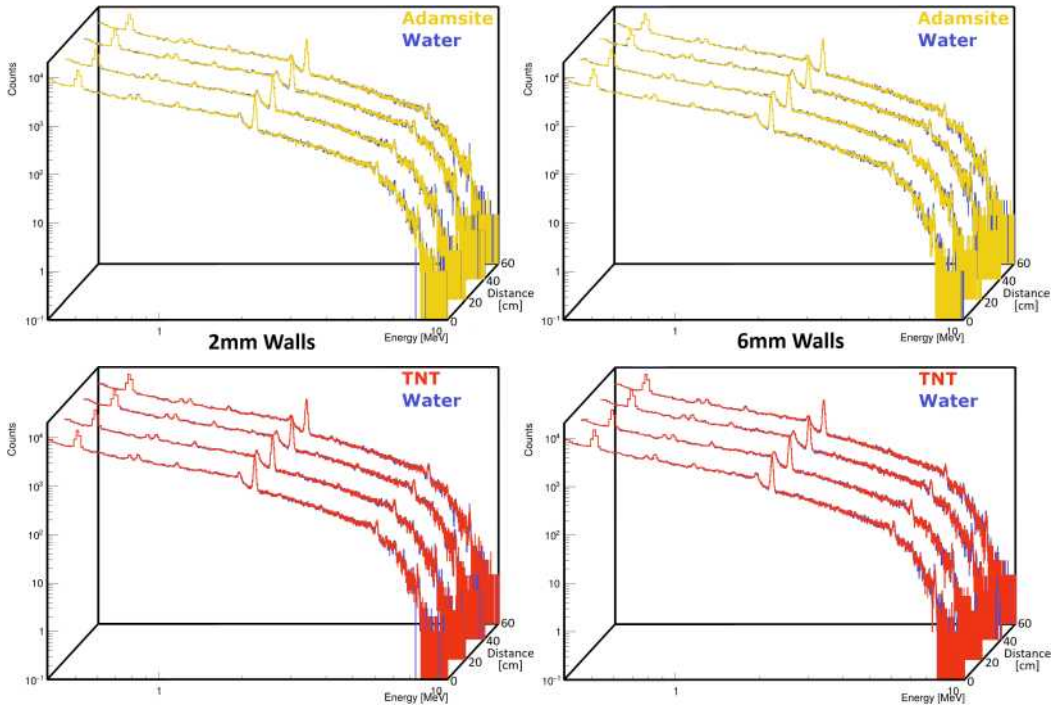

Figure 8 Energy distribution of all event from the simulations with the projectile type of the target. It is shown for (yellow) Adamsite and (red) TNT with the (blue) Water distribution as the reference spectra for different distances between the target and the detection setup (0, 20, 40 and 60 cm) and for different thickness of the projectile walls (2 and 6 mm).

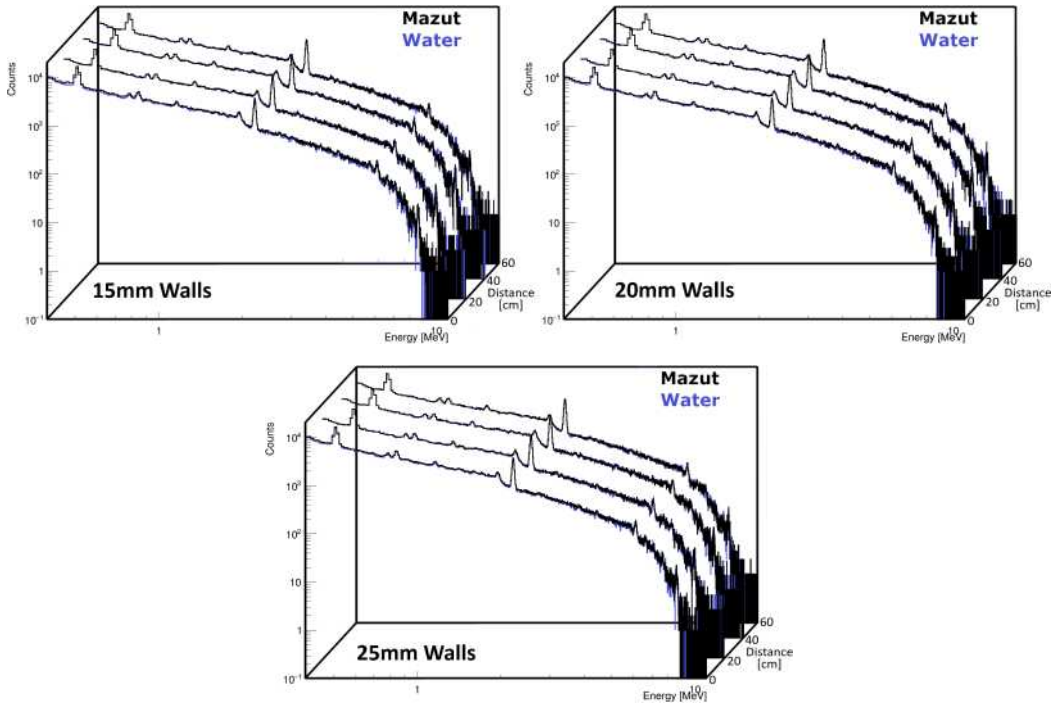

Figure 9 Energy distribution of all events from the simulations with the ship type of the target. It is shown for (black) Mazut with the (blue) Water distribution as the reference spectra for different distances between the

target and the detection setup (0, 20, 40 and 60 cm) and for different thickness of the projectile walls (15, 20 and 25 mm).

Additionally, for thicker target walls, a clear enhancement of the energy distribution at lower energies (below 1.5 MeV) is seen, originating from secondary radiation after the neutron interacts with the wall material - iron. Regarding the distributions of the photon arrival time at the detector after neutron emission, visible in **Figure 10** and **11**, there is no clear effect of the distance of the target from the detector or the thickness of the target walls. However, it is worth pointing out the significant enhancement of the tail with long times for mazut when the detector is very close to the target, coming from the increased chance of the capture process (which on average takes much longer due to the need for neutron thermalization), especially by carbon isotopes, in which mazut is rich.

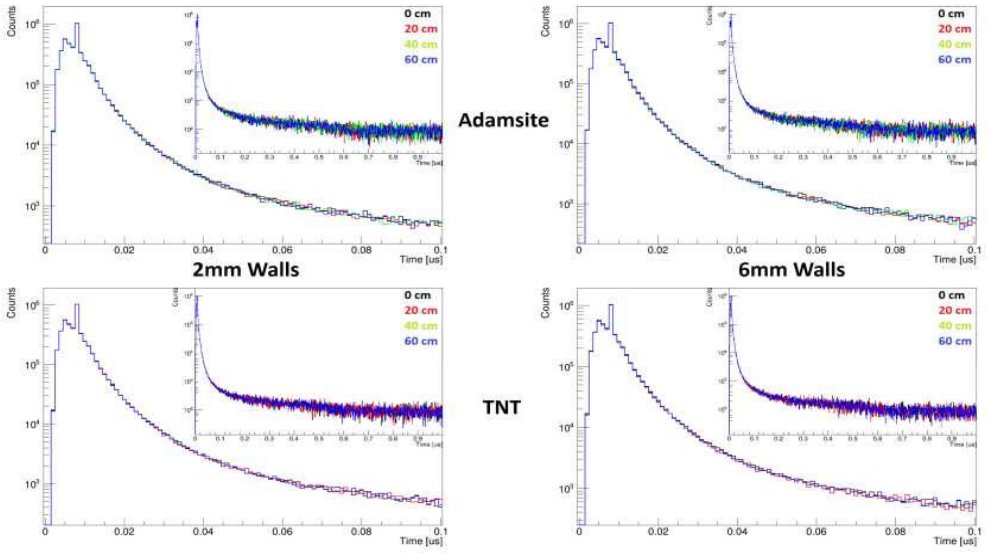

Figure 10 Time distribution of all events from the simulations with the projectile type of the target. It is shown for Adamsite and TNT for different distances between the target and the detection setup (0, 20, 40 and 60 cm) and for different thickness of the projectile walls (2 and 6 mm).

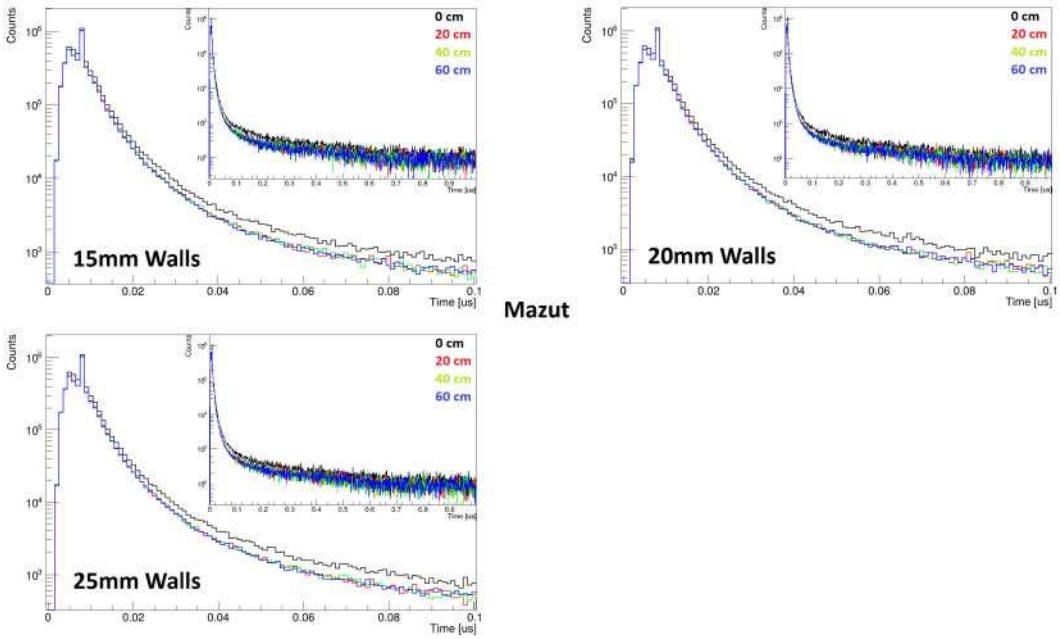

Figure 11 Time distribution of all events from the simulations with the ship type of the target. It is shown for Mazut for different distances between the target and the detection setup (0, 20, 40 and 60 cm) and for different thickness of the projectile walls (2 and 6 mm).

After fitting the energy distributions, the most prominent energy lines were extracted and divided by the intensity of the reference line - hydrogen (2.223 MeV) to eliminate the dependence on the number of events collected per distribution. The results for each material can be seen in **Figure 12 - 16**. It's easy to see how the 0.511 energy line clearly separates simulated materials from water, especially when comparing the situation when the target is very close to the detector (0 cm) and when moving away from the target. Additionally, the iron line (0.85 MeV), originating primarily from the target walls and ROV material, also varies with distance and target wall thickness, suggesting the potential use of this line for characterizing the container in which the object being tested is located. The remaining lines do not show any clear separation properties between water and the studied material, although perhaps a larger number of simulated events could strengthen the distinction from the chlorine (0.79, 1.17, 1.95 MeV) or oxygen (3.79, 6.11 MeV) lines present in large amounts in water.

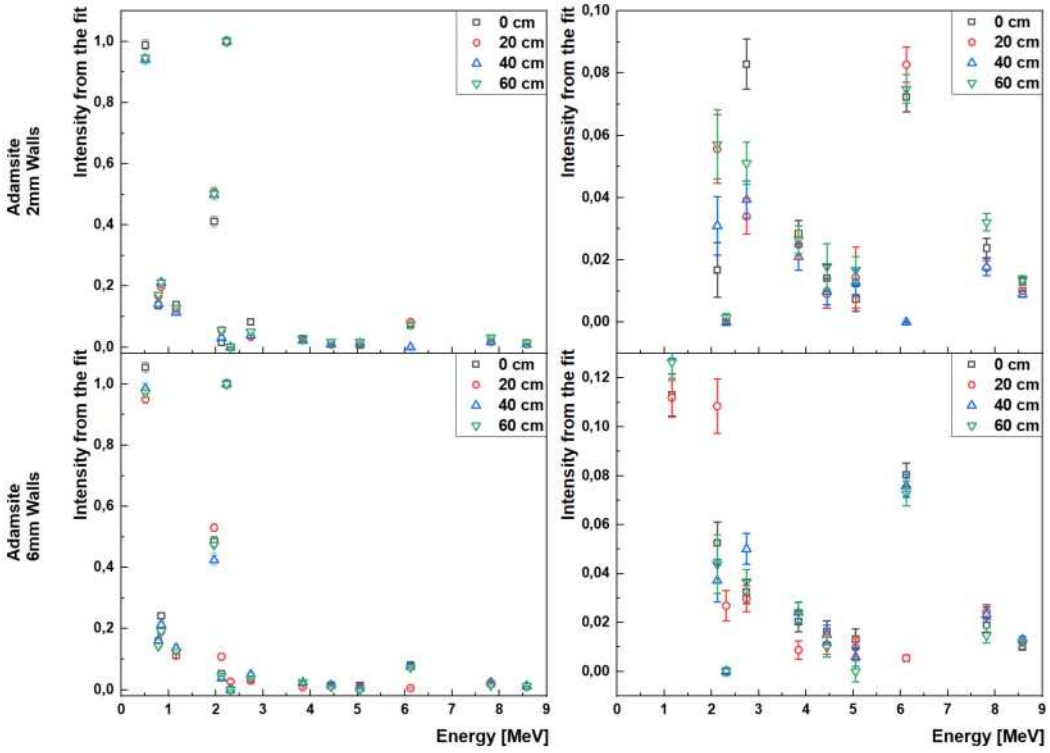

Figure 12 Fitted intensities of the most prominent lines, divided by the intensity of the hydrogen line (2.223 MeV) for Adamsite (left) in the full range and (right) in the narrowed range to lower intensities for two thicknesses of the walls - 2 and 6 mm.

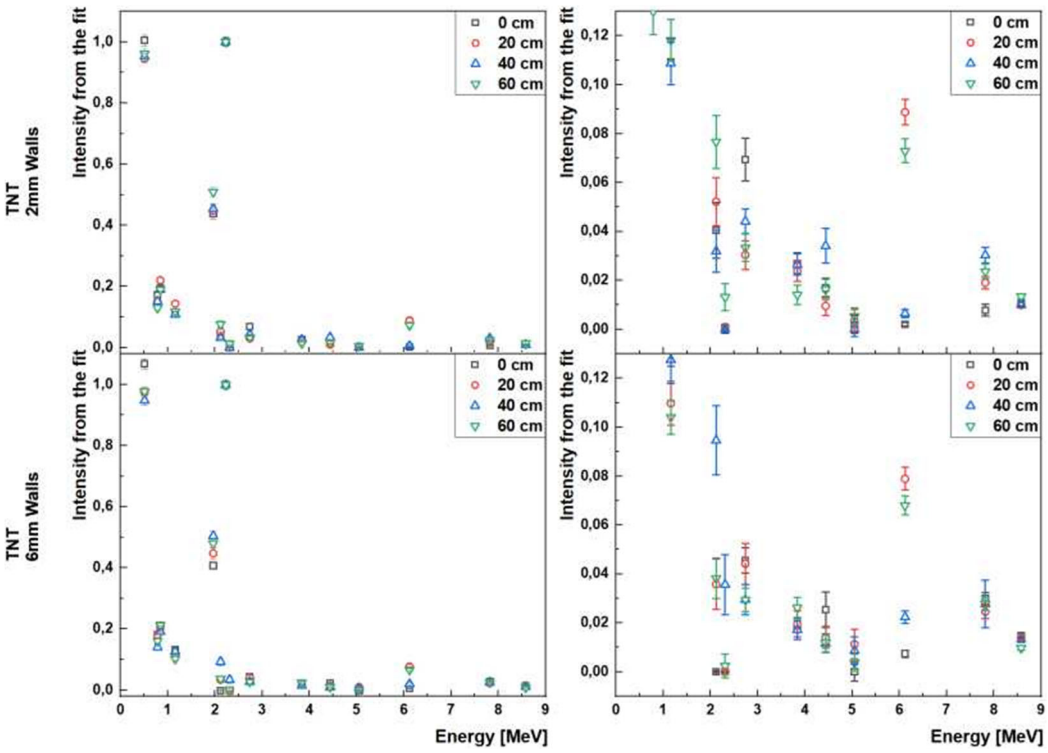

Figure 13 Fitted intensities of the most prominent lines, divided by the intensity of the hydrogen line (2.223 MeV) for TNT (left) in the full range and (right) in the narrowed range to lower intensities for two thicknesses of the walls - 2 and 6 mm.

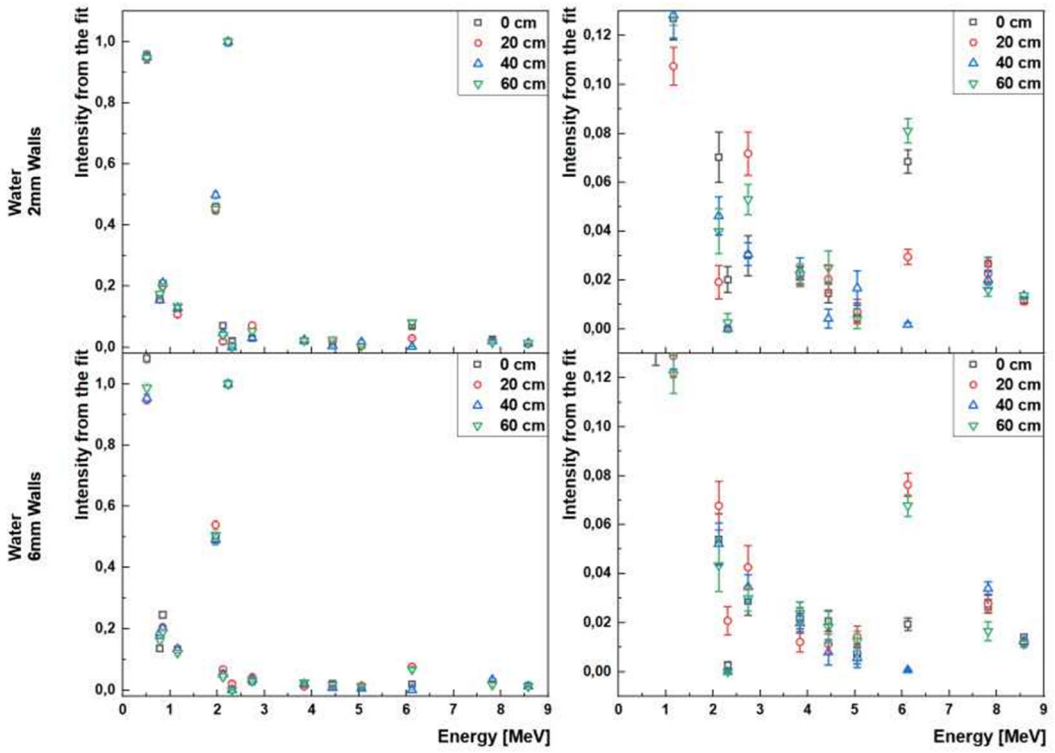

Figure 14 Fitted intensities of the most prominent lines, divided by the intensity of the hydrogen line (2.223 MeV) for Water (left) in the full range and (right) in the narrowed range to lower intensities for two thicknesses

of the walls - 2 and 6 mm.

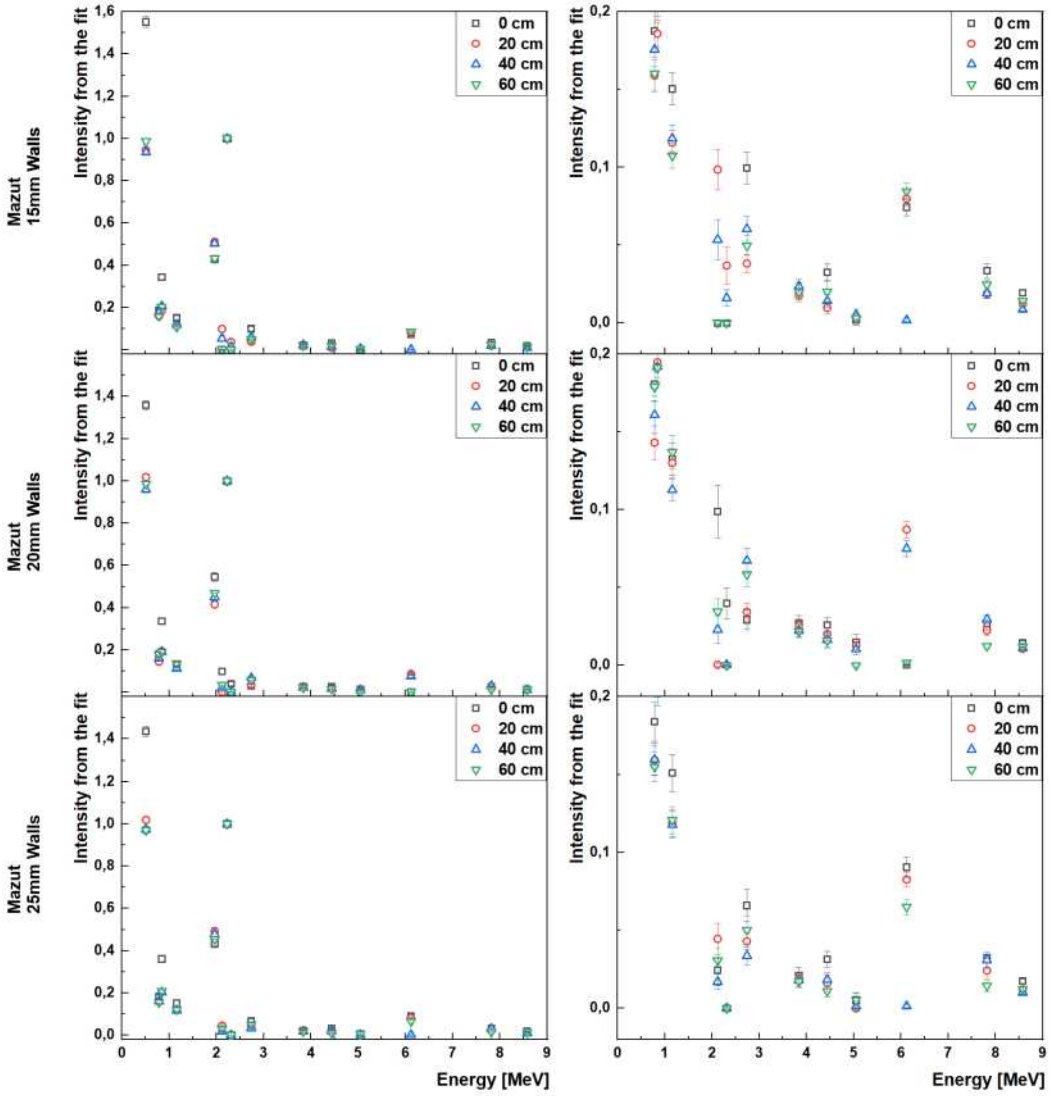

Figure 15 Fitted intensities of the most prominent lines, divided by the intensity of the hydrogen line (2.223 MeV) for Mazut (left) in the full range and (right) in the narrowed range to lower intensities for three thicknesses of the walls - 15, 20 and 25 mm.

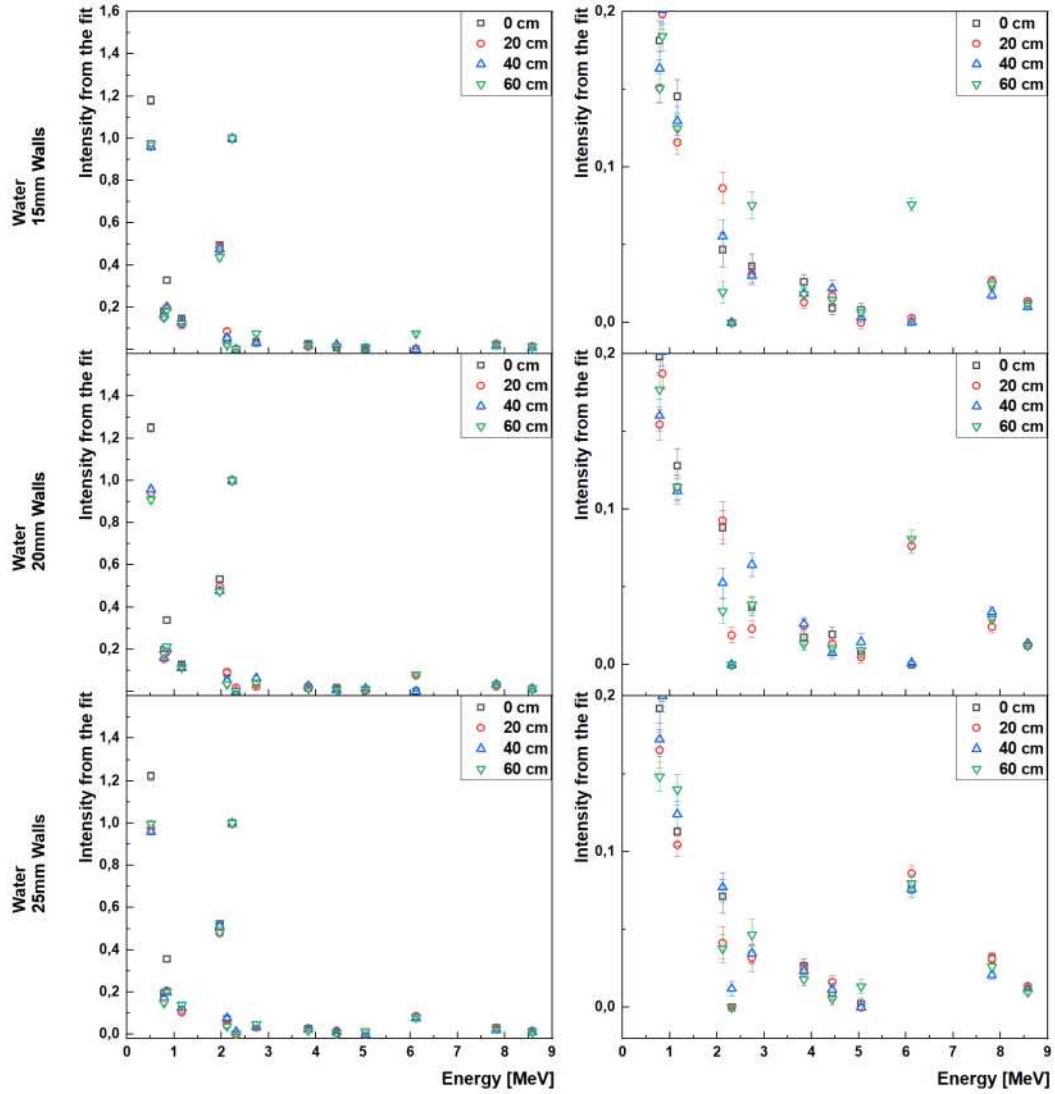

Figure 16 Fitted intensities of the most prominent lines, divided by the intensity of the hydrogen line (2.223 MeV) for Water (left) in the full range and (right) in the narrowed range to lower intensities for three thicknesses of the walls - 15, 20 and 25 mm.

The final part of the analysis was based on estimating the correlation between the intensities of the fitted lines and the detector-target distance and wall thickness. For this purpose, two types of lines were selected: those that positively distinguish water (the previously mentioned chlorine and oxygen lines) and those that negatively distinguish water (the 0.511 MeV line and the iron lines - 0.85 and 2.74 MeV). For each material and line type, the average intensity difference from the corresponding water intensity line was estimated, as in Figure 17 - 19. An exponential model was fitted to each dependence by estimating two main parameters - amplitude A and mean I, in accordance with the model formula:

$$y_o + A \exp(-d/I),$$

where y_o is background level, and d is the distance between the detector and the target. The model parameter results from positive and negative fitting are summarized in **Figure 20**. The obtained accuracy does not allow for drawing significant conclusions, but there is some potential for characterizing the container containing the tested substance based on the energy spectra of neutron

interactions. In fact, this may be possible by comparing the relative intensity of both positive and negative lines with the water, which is treated as a background material.

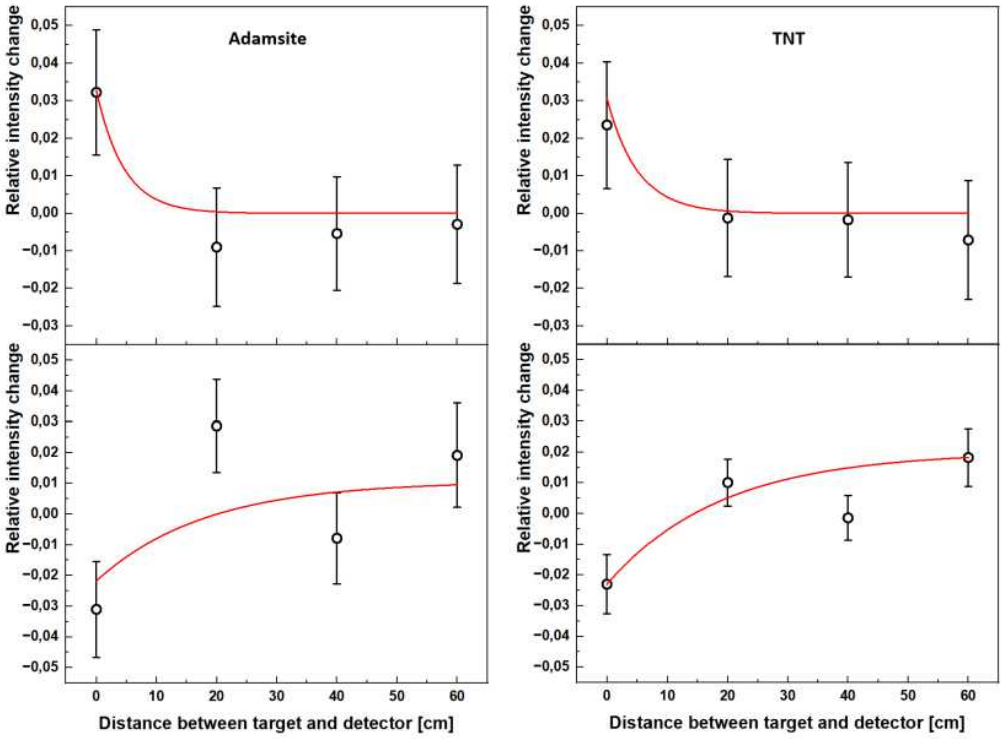

Figure 17 Change in intensity relative to water as a function of the distance of the object from the detection system for selected energy lines, for (left) Adamsite and (right) TNT for target with 2 mm thick walls. The energy lines have been divided into those giving (top) negative and (bottom) positive change. Fit function is the exponential decay model.

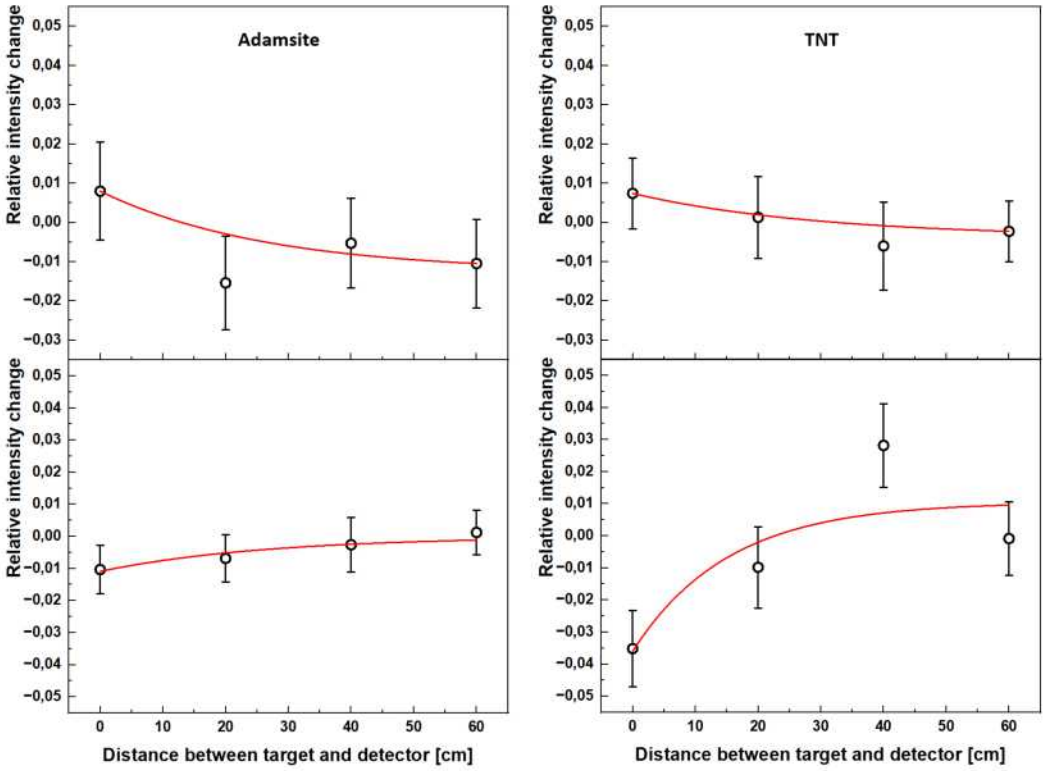

Figure 18 Change in intensity relative to water as a function of the distance of the object from the detection system for selected energy lines, for (left) Adamsite and (right) TNT for target with 6 mm thick walls. The energy lines have been divided into those giving (top) negative and (bottom) positive change. Fit function is the exponential decay model.

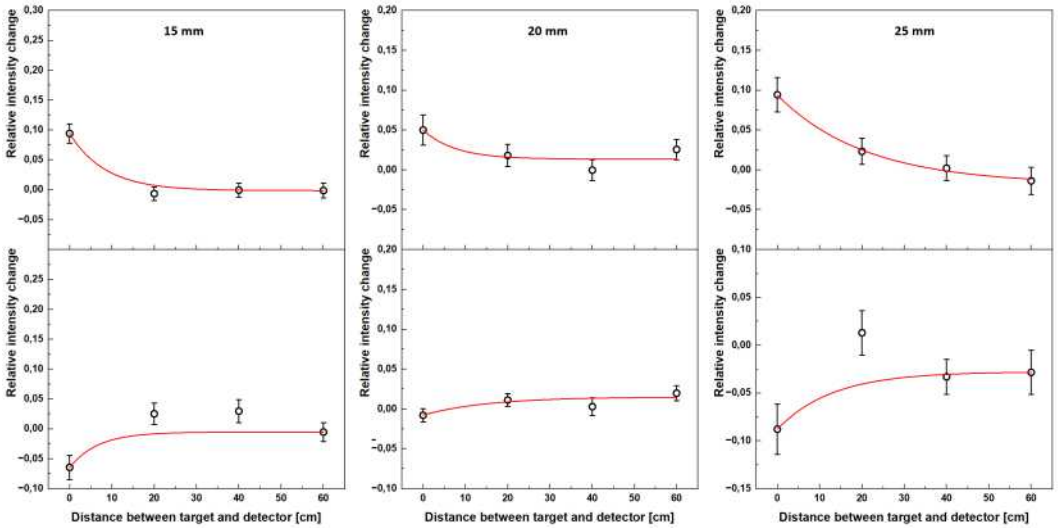

Figure 19 Change in intensity relative to water as a function of the distance of the object from the detection system for selected energy lines, for mazut for target with (left) 15 mm, (middle) 20 mm and (right) 25 mm thick walls. The energy lines have been divided into those giving (top) negative and (bottom) positive change. Fit function is the exponential decay model.

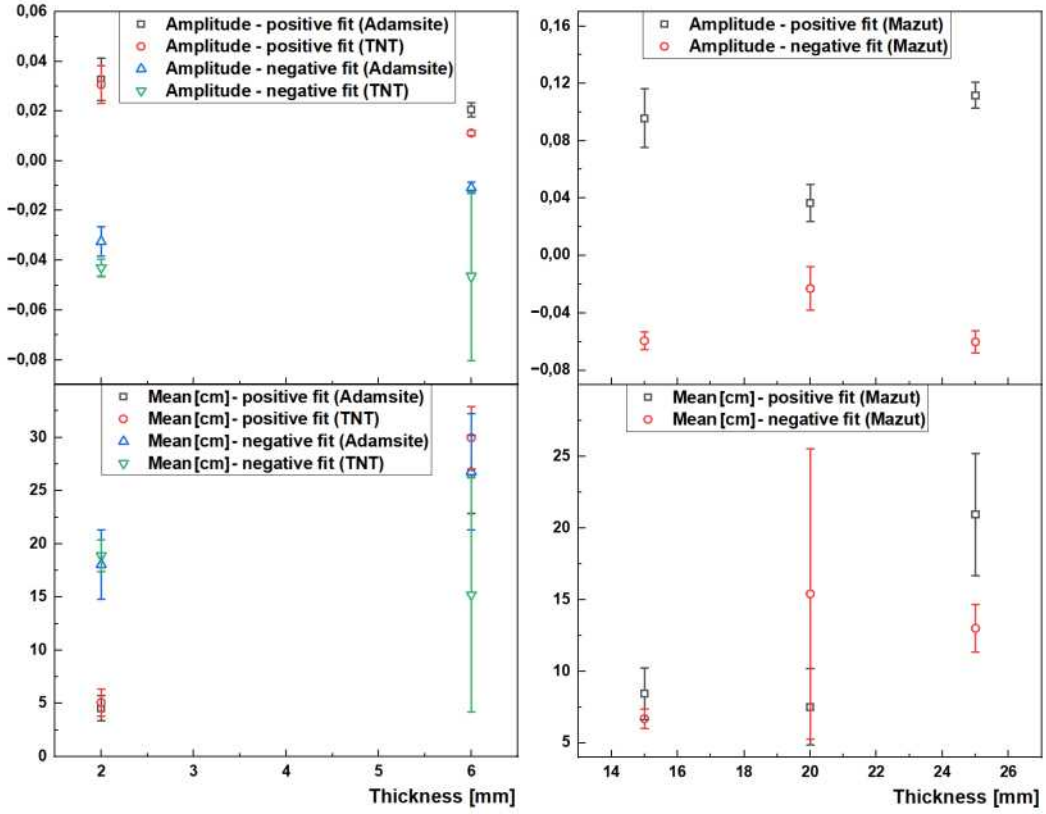

Figure 20 Model parameter results from estimating the correlation between the intensity difference relative to water and the distance between the detector and the target being tested.

3.2 Experimental results

The experimental part was conducted in laboratory conditions that simulated, to some extent, the aquatic environment. It focused on the influence of the water layer and container wall thickness on the NAA signal measured for the γ lines characteristic of the main elements that build the hazardous materials stored at the bottom of the Baltic Sea: hydrogen, oxygen, nitrogen, chlorine, and carbon. As a surrogate of the explosive substances, 1 kg of melamine (C3H6N6) was irradiated, while about 2 kg of NaCl was used to generate the signal for chlorine present in the mustard gas and Clark 1 and adamsite. A sample of around 3 kg of a seabed contaminated with synthetic fuel, taken from the vicinity of the Stuttgart wreck, was also studied in view of the detection of the fuel deposited in shipwrecks. An AmBe neutron source, available in the Institute of Physics of the Jagiellonian University, was used for initial calibration of the two γ-rays spectrometers, which were then operated in the next stage of the project. We have tested two scintillator detectors consisting of a Hammamatsu R7724-100 and 2"x2" LaBr3:Ce and CeBr3, respectively. The initial calibration and optimization were done with elemental sources (137Cs, 22Na and 60Co) and with the AmBe neutron source for energies up to 6.13 MeV. The working high voltage of the photomultipliers was set to 700 V and 800 V for the LaBr3:Ce and CeBr3 detectors, respectively. Both spectrometers were connected to the Nucliflare DAQ system, which, at the same time, was supplying the HV to the two photomultipliers and registering their signals in the Multi-Channel Analyser mode. All the samples were activated using the fast neutron generator IGN-14 operating in the Institute of Nuclear Physics PAS, with detectors in fixed positions with respect to the generator target, as shown in **Figure 21.** The measurements were done with two experimental setups. The conditions in the aquatic environment were simulated by layers of tap water 20 cm thick which were placed in front of the studied samples on the side of one of the detectors and the neutron generator (**Figure 21a**)**.** The detectors were placed 20 cm and 33 cm from the sample for the CeBr3 and LaBr3:Ce, respectively. Such a configuration enabled subsequent

simulations of the real conditions and measurement of the neutron capture signal not affected by the layer of water. The second experimental setup is shown in **Figure 21b** where the water tanks were removed and detectors were moved toward the sample (both detectors were placed around 3 cm from the Baltic Sea bottom sample). These measurements maximize the neutron inelastic scattering signal which was then compared with the signal for neutron capture reactions. All the measurements were compared with the γ -rays distribution obtained for water without any sample. These measurements were also used to additionally check the linearity of the used detectors. Joint results of this calibration are shown in **Figure 22**. As one can see, the response of both spectrometers are linear in a broad range from few hundreds of keV to more than 6000 keV (the carbon and chlorine characteristic γ -rays). Based on the obtained linear parametrizations, the detectors were calibrated energetically, and the further analysis was focused on the measured characteristic γ -rays intensities. The energy spectra measured with the water environment simulating setup (**Figure 21a**) are shown in **Figure 23a** and b for both detectors used in these studies. To obtain statistically precise shapes of the γ characteristic lines each of the measurements was performed for 20 minutes. As expected, these distributions do not differ significantly, and thus, the line intensities themselves are not optimal observables. Instead, to compare the results for different materials we have used the elemental rations. Among many possibilities the normalization by the hydrogen line (2223 keV) appeared to be the optimal one, since it appears in all the spectra and is highly populated (the statistical uncertainty of its intensity is small). The obtained values of the ratios can be found in **Table 1**.

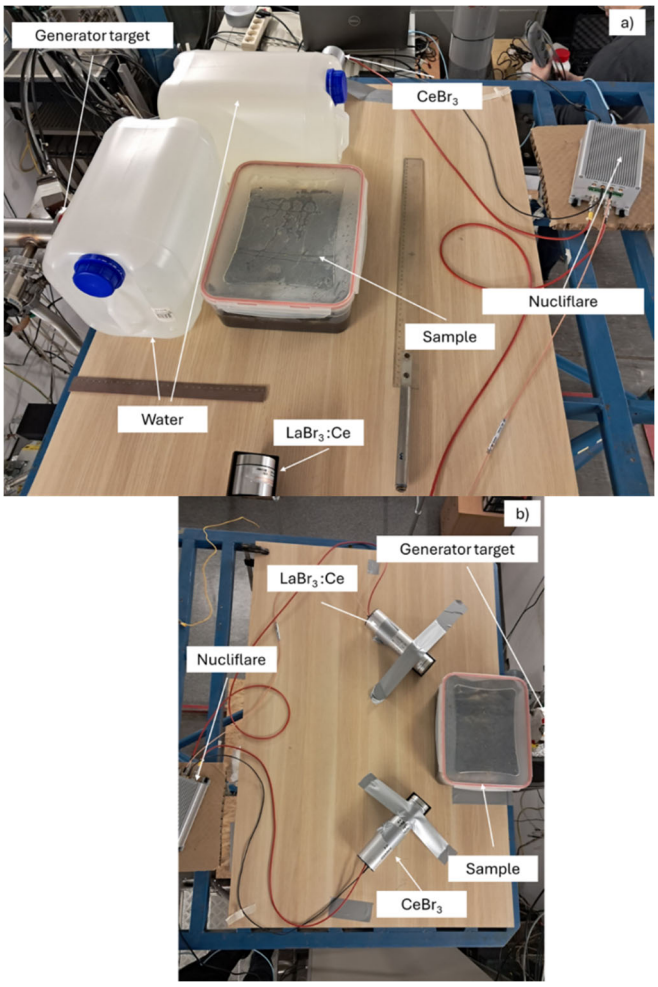

Figure 21 Picture of the experimental setup used in the measurements simulating an aquatic environment **(a)** and without water **(b)**, enhancing the neutron scattering.

Table 1 Intensity ratios of the selected elemental lines normalized to the hydrogen signal, obtained with the LaBr3:Ce detector for Melamine, sea bottom sample and water. Columns labelled with "2 mm" contain results obtained using a 2 mm steel cover (and water layer) in front of the sample simulating the munition shell. Data labelled "w/o water" were measured with the detector exposed to the sample without any barriers.

Energy MeV	Melamine w/o water	Sea bottom w/o water	Melamine	Sea bottom	Melamine 2 mm	Sea bottom 2 mm	Water
0.511	3.611(29)	3.292(26)	2.728(26)	2.383(12)	3.016(51)	2.508(17)	1.983(5)
0.79 (Cl)	0.611(8)	0.626(8)	0.464(6)	0.279(5)	0.524(45)	0.327(6)	1.681(5)
0.85 (Fe)	3.109(25)	2.990(23)	2.316(22)	1.84(1)	2.695(47)	1.99(2)	1.87(1)
1.17 (Cl)	0.480(8)	0.871(8)	0.395(7)	0493(5)	0.26(5)	0.529(6)	1.34(80)
1.95 (Cl)	0.377(7)	0.339(6)	0.372(6)	0.262(6)	0.469(43)	0.329(5)	1.22(1)
2.12 (Cl)	0.0006(4)	0.0473(32)	0.066(1)	0.0043(1)	0.087(24)	0.00004(1)	1.059(3)
2.31 (N)	0.144(5)	0.162(8)	0.1117(17)	0.0621(17)	0.0549(12)	0.0578(19)	1.411(3)
4.44 (C)	0.199(4)	0.1408(33)	0.096(2)	0.107(3)	0.095(2)	0.090(2)	0.612(2)
5.11 (N)	0.1753(32)	0.123(3)	0.112(2)	0.107(2)	0.128(24)	0.120(3)	0.795(3)
6.12 (O)	0.255(3)	0.191(3)	0.171(3)	0.205(3)	0.171(13)	0.184(3)	0.741(3)
7.79 (Cl)	0.000070(6)	0.0096(7)	0.0550(15)	0.0450(15)	0.016(7)	0.0101(7)	0.0392(4)

As one can see, all the studied surrogate materials are can be distinguished from the reference substance: water. The influence of 20 cm layer of water and steel barrier can be also seen for most of the lines. The elemental ratios tend to the same values for melamine and heavy fuel, however the differences can be seen, especially for the annihilation line (0.511 MeV). The carbon signal gives much smaller sensitivity which already with 2 mm of steel does not allow for the separation of melamine and heavy fuel. The chlorine lines, which, in general, constitute a measure of background, can be also used to this purpose. This points to the fact, that the sea bottom sample contains small amounts of water and chlorine. Their origin was confirmed with the NaCl measurements. A well-measured background line appears at 0.85 MeV and originates from Fe. The intensity ratios increases after adding the 2 mm of steel. This effect can be also seen in the measurements without water (**Figure 21b**), where we made a series of similar measurements to assess the influence of water on the signal of the neutron inelastic scattering. The energy spectra obtained in this part of the experiment were shown in **Figure 24**. The corresponding elemental rations were gathered in **Table 2**.

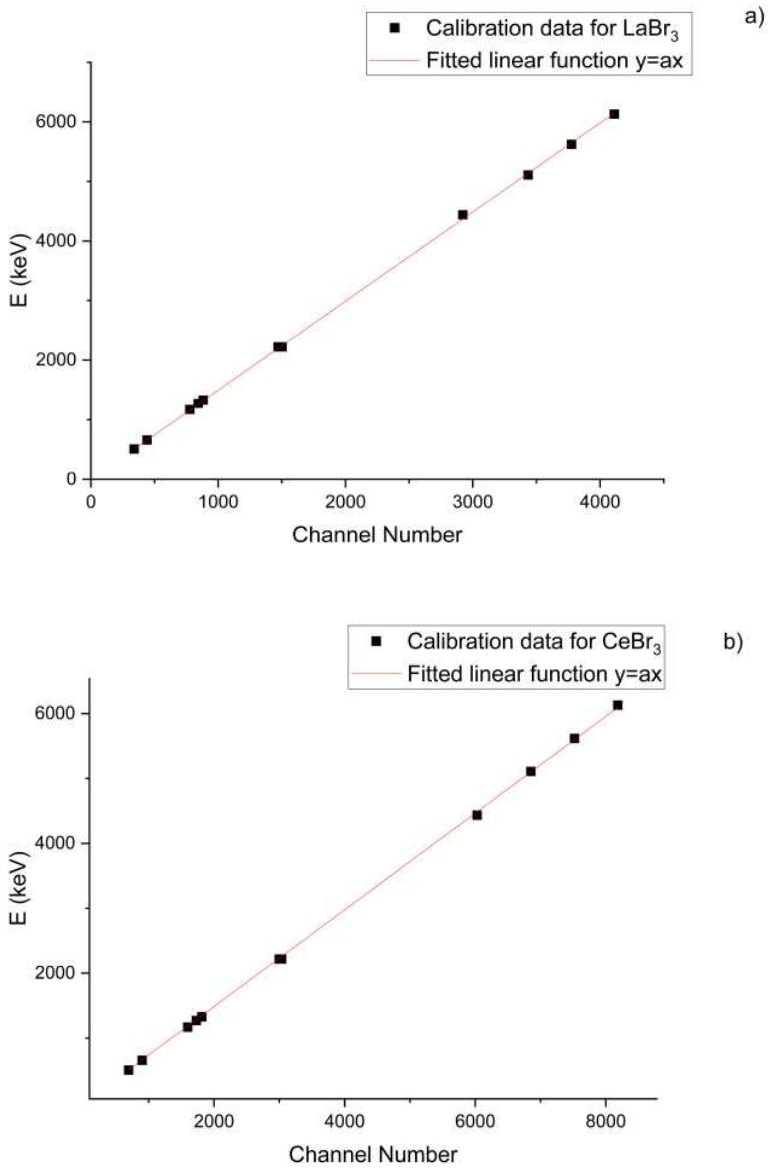

Figure 22 Calibration curves obtained for the $LaBr_3$:Ce **(a)** and $CeBr_3$ **(b)** detectors showing a very good linearity in a broad range of energies of the measured γ-rays. Data points for energies up to about 4400 keV were obtained using the elemental sources, while the high energy points were measured irradiating water with the 14.1 MeV neutron generator. The fitted calibration constants amount to a = 1.4951 ± 0.0038 keV/channel and a = 0.74466 ± 0.0017 keV/channel for the $LaBr_3$:Ce and $CeBr_3$ detectors, respectively.

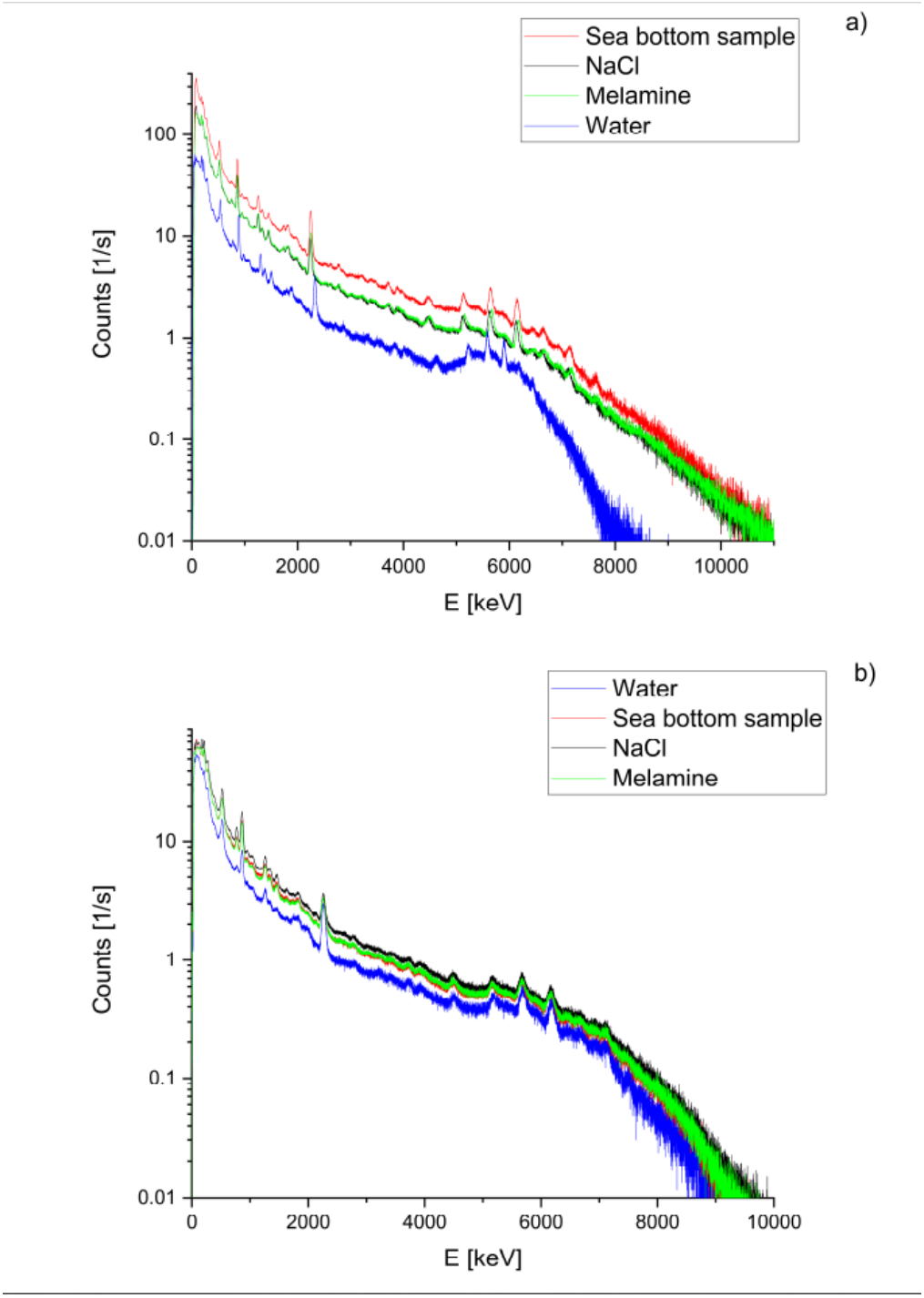

Figure 23 Energy distributions obtained experimentally with the $LaBr_3$:Ce **(a)** and $CeBr_3$ **(b)** detectors for all the studied surrogate materials.

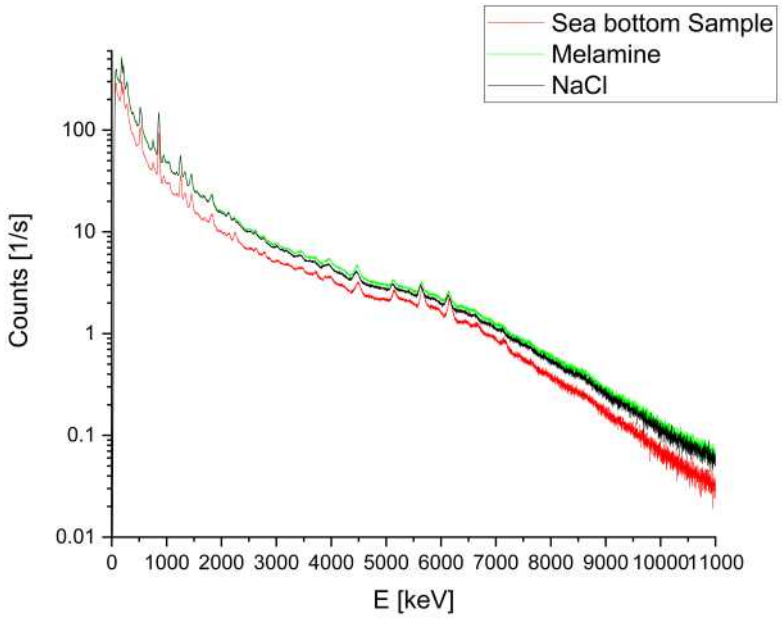

Figure 24 Energy distributions obtained experimentally with the $LaBr_3$:Ce detectors for all the studied surrogate materials without water for neutron thermalization.

Table 2 Intensity ratios of the selected elemental lines normalized to the hydrogen signal, obtained with the $LaBr_3$:Ce detector for Melamine, Sea bottom sample, and NaCl without water (**Figure 21b**).

Energy [MeV]	Melamine	Sea bottom	NaCl
0.511	18.65(9)	4.79(56)	4.78(44)
0.79 (Cl)	6.68(4)	0.97(12)	1.45(2)
0.85 (Fe)	22.9(1)	5.34(62)	5.72(5)
1.17 (Cl)	0.64(1)	0.26(4)	1.75(2)
1.95 (Cl)	0.0	0.11(2)	0.93(1)
2.12 (Cl)	0.383(7)	0.23(3)	1.53(2)
2.31 (N)	0.68(2)	0.54(7)	1.40(2)
4.44 (C)	0.943(1)	0.29(4)	0.836(8)
5.11 (N)	0.272(6)	0,11(2)	1.02(1)
6.12 (O)	0.362(6)	0,17(2)	0.612(7)
7.79 (Cl)	0.614(8)	0,009(1)	0.098(2)

The presence of chlorine is clearly seen in the data for NaCl, even if we did not thermalize neutrons with water. The same effect can be seen for melamine, containing relatively high number of nitrogen atoms which can be detected mainly through neutron capture. Without water the background line of iron also increased significantly. At the same time, the neutron inelastic scattering lines (C and O) also increased with respect to the previous measurements. At the same time we observed increased count rates in the LaBr3:Ce. Also the number of pileups detected by the DAQ system was highly increasing. This effect is manly connected to the activation of the detector material (mainly Br atoms) which was also deteriorating to some extent its energy resolution.

4. Conclusions

Based on the research and field trials conducted during the MODUM project, there is conclusion that The implementation of a deployable headspace GC–MS instrument proved highly effective for the real-time detection of sulfur mustard-related cyclic degradation products in marine sediment. These field findings were consistently validated by subsequent high-precision analysis at reach-back laboratories, demonstrating that this mobile method is a reliable tool for identifying sulfur mustard-affected objects during active maritime surveys. In contrast, the capillary electrophoresis (CE) method, while successfully validated in a controlled laboratory setting, demonstrated a need for further optimization before it can be effectively integrated into standard on-board analytical workflows. Future development for on-board techniques should prioritize the detection of arsenicals. Establishing a robust field-ready capability for arsenic-based agents would allow monitoring teams to cover both primary classes of chemical agents—mustards and arsenicals—simultaneously during a single cruise.

Results of NAA analysis showed, that sensor consisting of a compact neutron generator (e.g. Thermofishser MiniGeen with dimensions of 10.8 x 20.3 x 25.4 cm3 and weight of about 7 kg) and γ-rays spectrometer based on the scintillating crystals (e.g. LaBr3:Ce with dimensions 5.5 cm (dia.) x 25 cm) will be able to detect even relatively small amounts of the illicit materials (few kg) from a distance of dozen or so to several dozen centimeters. With a low-power DAQ system allowing for both, the HV supply to the detector (e.g. Nucliflare, and for registration of γ- radiation signals, it could be integrated with a ROV and operated remotely on site. The results show, however, that the performance of the identification using such a NAA-based sensor depends on the distance of the neutron generator and γ--rays detector from the inspected object. Both, Monte Carlo simulations, and experiment, showed a big influence of water, in which neutrons are moderated and scattered. The 20 cm thick layer simulated in the experiment appeared to be already suppressing part of the 14.1 MeV neutron flux from the used generator. This conclusion is supported by the presence of the increased thermal neutron signal for measurements without water. This means, that the signal of neutrons moderated in the sample itself was higher, than the one induced by the neutrons moderated in water (self-absorption of water is not negligible). The presence of ammunition shells also influence the signal of the illicit substances, but the effect is not as important, as the distance in water. Altogether, these two effects significantly decrease the sensitivity of the sensor, thus the measurements must be performed as close to the inspected object, as possible. In case of heavy fuel contained in wrecks, sensor may be magnetically attached to the side of the wreck. In this case the successful measurement may be performed for few tens of seconds (taking into account also the big amounts of fuel inside wrecks). For smaller objects the time of interrogation may be higher, depending on the signature which one needs to detect. From both parts of the research one can conclude, that the Cl lines at energies up to 6.13 MeV can be effectively measured even from a 20 cm distance. Also the annihilation γ-rays constitutes strong detection signal. Much weaker signal is seen for carbon and nitrogen. Here, the separation of neutron capture and inelastic scattering would significantly increase the sensitivity for the two mentioned elements. It would also separate signal of oxygen from the nitrogen and chlorine. This effect was demonstrated with the Monte Carlo simulations assuming a α particle detector tagging the time of the neutron generation and its direction. it should be noted, however, that such solutions are not yet available with the compact neutron generators. Instead, one can use only the triggered acquisition of the DAQ system using the neutron pulse generation signal. The increase of neutron inelastic scattering for measurements without water confirm, that the water layer thickness between the sensor and the inspected object plays important role. To some extent this effect may be reduced by using guides filled with air (as proposed in the SABAT project **(Silarski et al., 2023).** One should also take into consideration installation of the two main parts of the sensor, the neutron generator and the γ-rays detector on separate manipulating arms of the ROV, which may decrease the background count rates in the detector and shield it against neutrons activating its active part (mainly Br).

References

Allison J. et al., 2016. *Recent developments in geant4.* Nuclear Instruments and Methods in Physics Research Section A: Accelerators, Spectrometers, Detectors and Associated Equipment 835, 186. https://doi.org/10.1016/j.nima.2016.06.125

Amato E. et al., 2006. *R.E.D. C.O.D. Project: Research On Environmental Damage Caused By Chemical Ordnance Dumped At Sea.* Rome, Italy.

Bełdowski J. et al., 2016. *Chemical Munitions Search & Assessment-An evaluation of the dumped munitions problem in the Baltic Sea.* Deep-Sea Research Part II: Topical Studies in Oceanography 128, 85–95. https://doi.org/10.1016/j.dsr2.2015.01.017

Bełdowski J. et al., 2018. *Introduction.* In J. Bełdowski, R. Been, E. K. Turmus (Eds.), *Towards the Monitoring of Dumped Munitions Threat (MODUM)*. Springer, Dordrecht, 1-17. https://doi.org/10.1007/978-94-024-1153-9_1

BSH, Bundesamt für Seeschifffahrt und Hydrographie, 1993. *Chemical munitions in the southern and western Baltic Sea* – report by a federal/Länder government working group (in German) and cited references. Hamburg, Germany

Brun R., Rademakers F., 1997. *Root - an object oriented data analysis framework.* Nuclear Instruments and Methods in Physics Research Section A: Accelerators, Spectrometers, Detectors and Associated Equipment 389 (1-2), 81-86. https://doi.org/10.1016/S0168-9002(97)00048-X

Fish J. T., et al., 2010. *Practical crime scene investigations for hot zones.* CRC Press, Boca Raton

HELCOM, 1995. *Final Report of the ad hoc Working Group on Dumped Chemical Munition (HELCOM CHEMU)* to the 16th Meeting of the Helsinki Commission.

HELCOM, 2013. *Chemical Munitions Dumped in the Baltic Sea.* Report of the ad hoc Expert Group to Update and Review the Existing Information on Dumped Chemical Munitions in the Baltic Sea (HELCOM MUNI).

Jõul P., et al., 2015. *Development of a capillary electrophoresis method with direct UV detection for the analysis of thiodiglycol and its oxidation products.* Electrophoresis 36, 1202–1207. https://doi.org/10.1002/elps.201500038

Kubáň P., et al., 2011. *In situ determination of nerve agents in various matrices by portable capillary electropherograph with contactless conductivity detection.* Journal of Chromatography A 1218, 2618–2625. https://doi.org/10.1016/j.chroma.2011.03.006

Lang T., et al., 2018. *The Health Status of Fish and Benthos Communities in Chemical Munitions Dumpsites in the Baltic Sea.* In J. Bełdowski, R. Been, E. K. Turmus (Eds.), *Towards the Monitoring of Dumped Munitions Threat (MODUM).* Springer, Dordrecht, 129-152. https://doi.org/10.1007/978-94-024-1153-9_6

Li S. F. Y., 1992. *Capillary electrophoresis: principles, practice, and applications*. Journal of Chromatography Library, 52, Elsevier Science Publishers, The Netherlands.

Seiman A., et al., 2009. *A portable capillary electropherograph equipped with a cross-sampler and a contactless-conductivity detector for the detection of the degradation products of chemical warfare agents in soil extracts.* Electrophoresis 30, 507–514. https://doi.org/10.1002/elps.200800341

Silarski M., et al. 2023. Monte Carlo simulations of the underwater detection of illicit war remnants with neutron-based sensors. The European Physical Journal Plus 138, 751. https://doi.org/10.1140/epjp/s13360-023-04377-4

Söderström M., et al., 2018. *Chemical Analysis of Dumped Chemical Warfare Agents During the MODUM Project.* In J. Bełdowski, R. Been, E. K. Turmus (Eds.), *Towards the Monitoring of Dumped Munitions Threat (MODUM)*. Springer, Dordrecht, 71–103. https://doi.org/10.1007/978-94-024-1153-9_4

Stipa T., Paka V., 2006. *Modelling of ecological risks related to sea-dumped chemical weapons (MERCW).* Synthesis report of the available data. doi:10.1109/BALTIC.2006.7266161

Wilkinson I., et al., 2017. *Chemical weapon munitions dumped at sea: An interactive map*. Middlebury Institute of International Studies. https://nonproliferation.org/chemical-weapon-munitions-dumped-at-sea/

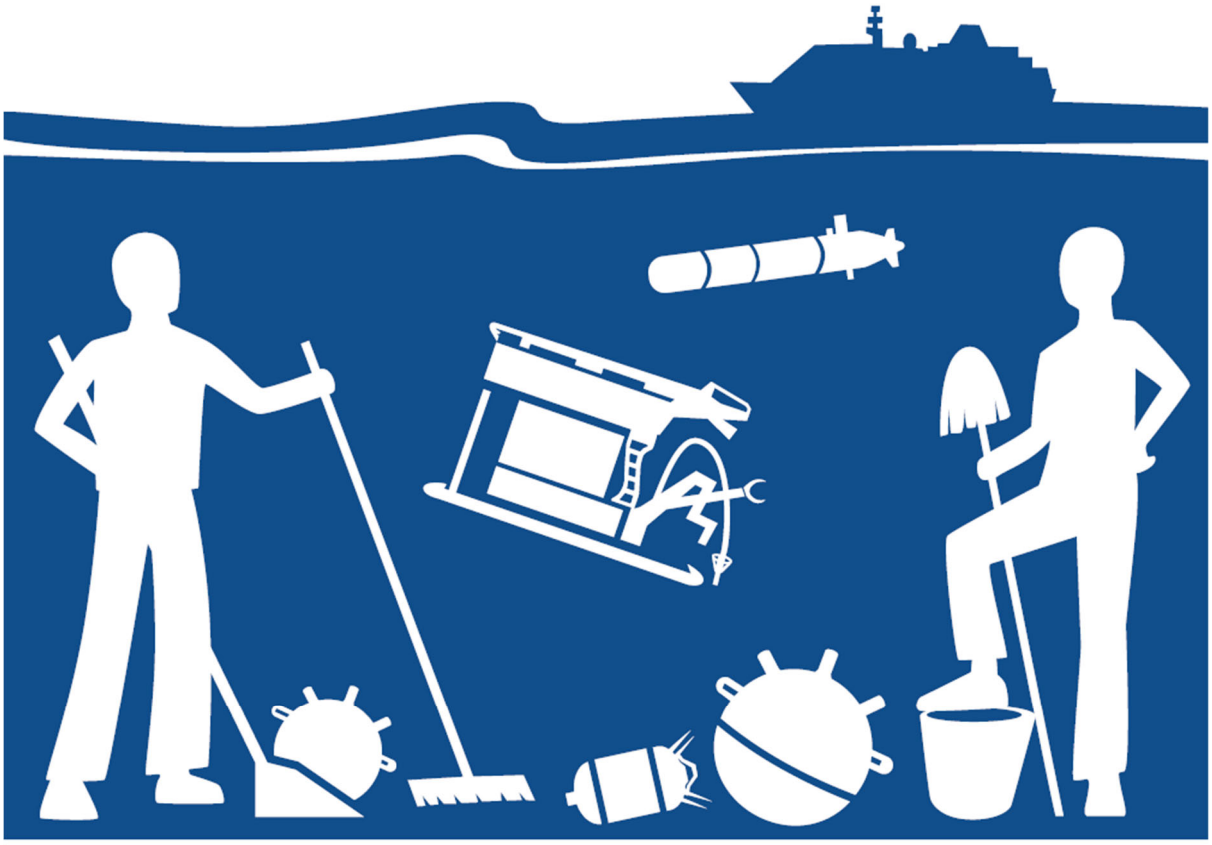

MMinE-SwEEPER

www.mminesweeper-munition.eu